arXiv:0708.4296v1 [astro-ph] 31 Aug 2007

Nuclear physics with spherically symmetric supernova models

M Liebendörfer, T Fischer, C Fröhlich, F-K Thielemann and S Whitehouse

Department of Physics, University of Basel, Klingelbergstr. 82, 4056 Basel, Switzerland

E-mail: matthias.liebendoerfer@unibas.ch

Abstract. Few years ago, Boltzmann neutrino transport led to a new and reliable generation of spherically symmetric models of stellar core collapse and postbounce evolution. After the failure to prove the principles of the supernova explosion mechanism, these sophisticated models continue to illuminate the close interaction between high-density matter under extreme conditions and the transport of leptons and energy in general relativistically curved space-time. We emphasize that very different input physics is likely to be relevant for the different evolutionary phases, e.g. nuclear structure for weak rates in collapse, the equation of state of bulk nuclear matter during bounce, multidimensional plasma dynamics in the postbounce evolution, and neutrino cross sections in the explosive nucleosynthesis. We illustrate the complexity of the dynamics using preliminary 3D MHD high-resolution simulations based on parameterized deleptonization. With established spherically symmetric models we show that typical features of the different phases are reflected in the predicted neutrino signal and that a consistent neutrino flux leads to electron fractions larger than 0.5 in neutrino-driven supernova ejecta.

PACS numbers: 26.30+k, 26.50.+x, 26.60+c, 97.60.Bw

1. Introduction

Stellar core collapse occurs towards the end of the evolution of massive stars when their iron cores grow beyond the critical mass supportable by the pressure of a nearly degenerate electron gas. The ensuing gravitational collapse of the inner core is an extreme example for the conversion of binding energy into (neutrino-)radiation [1]: The transition of the inner core of the supernova progenitor star to a compact neutron star makes an energy of few times 10^{53} erg available for the emission of neutrinos. This energy corresponds to a mass defect of the remnant ~ 0.1 $M_\odot$! The first (and so far only) detection of supernova neutrinos from SN1987A (summarised e.g. in [2]) recently celebrated its 20th anniversary. The detection of supernova neutrinos provides the most direct observational evidence for the link of a collapsing stellar core to a supernova explosion.

Computer models with spectral neutrino transport seem to agree on the general scenario of a delayed explosion (see [2] and references therein) in which we distinguish four different phases. During the *collapse phase*, the stellar core splits into a homologously collapsing subsonic inner core and the outer layers, which accrete with

supersonic infall velocities in the wake of the homologous collapse. The matter has an entropy $\sim 1\ k_B$/baryon and consists of heavy, neutron-rich nuclei. Electron captures and neutrino emission under these conditions are essential to determine the evolution of the electron fraction through collapse and the strength of the core rebounce in the *bounce phase*, which occurs when nuclear saturation density is exceeded at the center. Once nuclear density is reached the low compressibility of matter produces a stagnation wave traveling to the edge of the homologous core, where it faces the supersonic accretion. The wave turns into a shock which heats and dissociates the accreting matter. The sudden appearance of free protons in a neutrino-transparent regime leads to the emission of an energetic neutronization burst of electron neutrinos within $2 - 5$ ms after bounce. This concludes the bounce phase. The dynamic shock turns into a hydrostatically expanding accretion front, which, throughout the ensuing *accretion phase*, delimits the cold accretion flow from the hot dissociated matter piling up on the newborn protoneutron star (PNS). The fourth phase is the *explosion phase*, where a part of the hot accumulated matter drives the shock to larger radii into the outer layers, leading to a supernova explosion and the ejection of matter. Another part of the accumulated matter sinks onto the PNS or fills the space between PNS and ejecta in the form of a neutrino-driven wind. The explosion phase is thought to develop after an accretion phase lasting 500 ms or more, which is of order hundred times longer than the hydrodynamic bounce phase.

However, the obstinate difficulty to reproduce explosions in spherically symmetric models of core collapse and postbounce evolution stimulated the consideration of numerous modifications and alternatives to this basic scenario, mostly relying on multi-dimensional effects that could not be treated in spherical symmetry. To name only a few: It was discussed whether convection in the PNS could accelerate the deleptonisation and increase the neutrino luminosity [3]. The convective overturn between the PNS and shock front was shown to increase the efficiency of neutrino energy deposition [4]. Asymmetric instabilities of the standing accretion shock [5, 6] may help to push the shock to larger radii and g-mode oscillations of the PNS may contribute to neutrino heating by the dissipation of sound waves beween the PNS and the shock [7]. Moreover, it has been suggested that magnetic fields have an impact on the explosion mechanism (see e.g. [8]). Most of above-mentioned modifications of the explosion mechanism are essentially of a three-dimensional nature. In order to illustrate the complexity of the crucial accretion phase we show in Figure 1 a slice through a three-dimensional simulation of core collapse and postbounce evolution of a run described in more detail in [9]. Its input physics uses the Lattimer-Swesty equation of state [10] and a parameterisation of the neutrino physics for the collapse phase [11]. The treatment of neutrino cooling and heating in the postbounce phase is under development based on multi-group diffusion, but has not yet been successfully applied in this high-resolution run with 600^3 zones.

Initially, spherically symmetric supernova models were the most realistic among all feasible computer representations of the event. With increasing observational evidence for the complexity of the explosions (e.g. [12]) their primary purpose shifted from a realistic representation to the identification and understanding of the basic principles of the explosion mechanism. After the emergence of axisymmetric simulations with sophisticated and computationally intensive spectral neutrino transport [13, 14] spherically symmetric models still have several assets. In the following we describe selected applications of spherically symmetric models related to nuclear and weak interaction input physics.

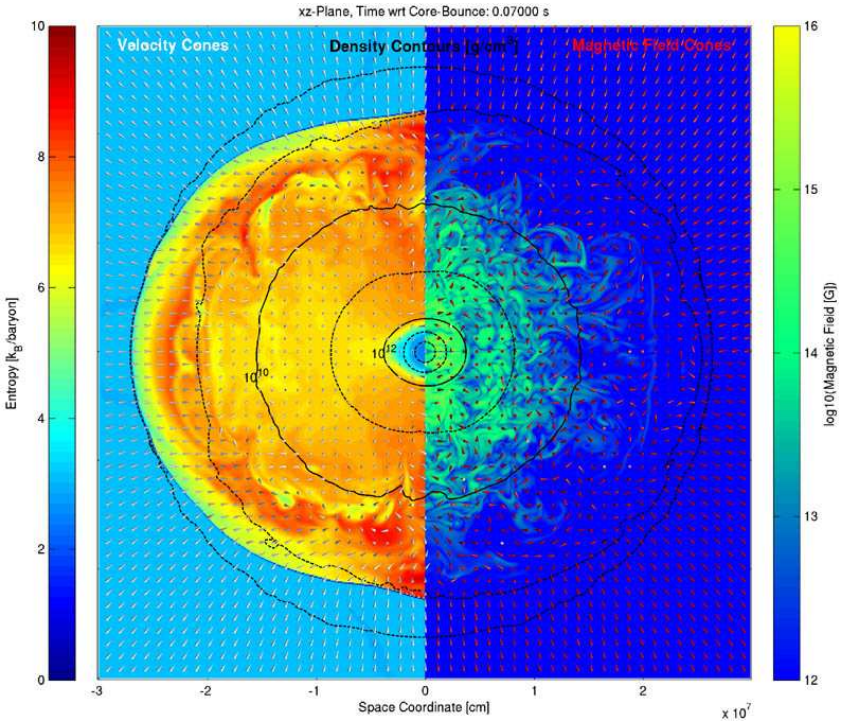

Figure 1. Illustration of the early accretion phase in a three-dimensional simulation with parameterized neutrino physics [9]. Density contours are drawn as black lines. The colour on the left hand side indicates the specific entropy and the cones the direction of the velocity. The colour on the right hand side refers to the magnetic field strength and the cones to its direction. The cool high-density interior of the PNS and the hot low-density accreted matter behind the standing accretion front are clearly distinguishable.

2. Conditions obtained with GR spectral neutrino transport

The complete general relativistic (GR) Boltzmann equation for neutrino transport has so far only been solved in spherically symmetric dynamical simulations [15, 16, 17]. Some of the GR effects have less effect on the explosion mechanism (e.g. the bending of neutrino trajectories by the PNS) than others (e.g. the GR effects included in the hydrostatic Tolman-Oppenheimer-Volkoff equation). Hence, accurate results can be obtained by the careful design of approximations [18]. But spherically symmetric simulations are not only useful as a testbed for approximations and comparisons [19], they can also provide a clearly arranged foundation to determine the conditions achieved in supernova simulations and to distinguish and study the input physics in different regimes. Figure 2 shows an overview of the conditions achieved in a simulation of the collapse, bounce, and explosion of a 20 $M_\odot$ star (model B05 in [20]). Figure 2a shows that the four phases of the supernova scenario involve quite distinct regimes of conditions. The conditions can be subdivided into three different regimes: The lower dark branch reaching from low densities up to nuclear density corresponds to cold infalling matter containing heavy ions. Its electron fraction in Figure 2b follows during infall the dark branch reaching from $Y_e = 0.5$ to $Y_e \sim 0.3$.

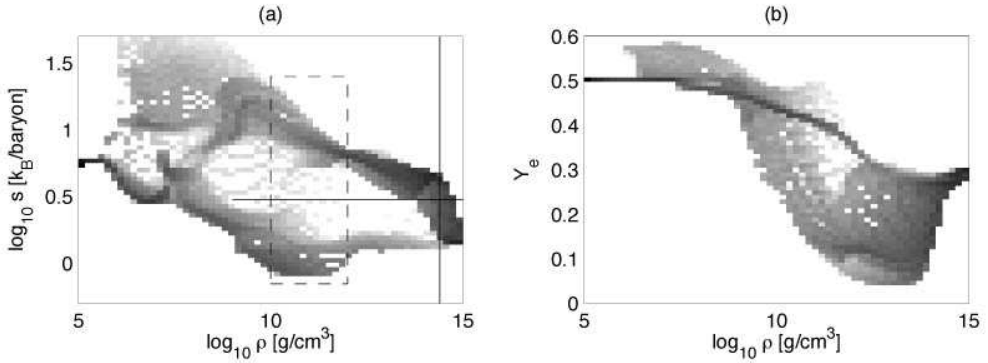

Figure 2. Overview of the conditions achieved in a simulation of the collapse, bounce, and explosion (artificially induced) of a 20 $M_\odot$ star. Shown are two histograms of the occurence of conditions as function of density ρ, specific entropy s and electron fraction Y_e. The shading of a given bin corresponds to $\log_{10}\left(\int dm\,dt\right)$ in arbitrary units, where the integral over mass is performed over the mass dm of matter whose thermodynamic state at a given time falls into the bin. The integral over time extends over the duration of a simulation. Hence, regions of dark shading correspond to states that are assumed by considerable mass for an extended time, while light or absent shading corresponds to conditions that are rarely assumed in the supernova simulation. The vertical black line indicates nuclear density. The horizontal black line indicates an entropy of 3 k_B/baryon beyond which ions are dissociated. In Figure 2a, it clearly separates the conditions of cold infalling matter on the lower branch from the conditions of hot shocked matter on the upper branch.

The matter beyond the nuclear density threshold in Figure 2a corresponds to bulk nuclear matter in the interior of the PNS. As one can see from Figure 2b it does not significantly deleptonize during the simulation because of the short mean free paths and correspondingly long diffusion times of the neutrinos at high density. As soon as infalling matter is hit by the accretion shock, its entropy jumps to the upper edge of the upper branch while its Y_e drops by enhanced electron capture in the dissociated regime. The darker tinted cloud around the density of 10^{10} g/cm^3 reaches entropies between 10 and 30 k_B/baryon by neutrino heating between the PNS and the standing accretion shock. The lighter tinted region toward lower densities and higher entropies indicates conditions during matter ejection. In Figure 2b part of the ejected matter assumes conditions with $Y_e > 0.5$ as we will discuss later.

3. Sensitivity of models to input physics changes

The exchange of lepton number and energy in the models is given by weak interaction rates between different neutrino flavours and matter. The latter is assumed to be in thermodynamic and nuclear statistical equilibrium except for the infalling outer layers and expanding ejecta. The effective weak interaction rates increase with increasing baryon density until the opacity reaches a level where the neutrinos diffuse away more slowly than they are produced. The rates then become Pauli-blocked. Hence there is a range of maximum importance of the weak interaction rates at densities around the neutrinospheres ($\sim 10^{10} - 10^{12}$ g/cm^3). The intersection of this density range (dashed box) with the two branches identified in Figure 2a leads to two important

regimes for weak interactions: The conditions on the lower branch at ($s \sim 1, Y_e \sim 0.35$) assumed in infalling layers during collapse, and the conditions on the upper branch at ($s \sim 10, Y_e \sim 0.1$) assumed in the hot mantle of the PNS during the accretion phase. Traditional treatments of the weak interaction rates in supernova simulations [21] recently received updates in both regimes. It was recognized that electron captures on nuclei (and not protons) provide the dominant deleptonization mechanism during collapse, even if the corresponding Gamov-Teller transitions seem forbidden in the oversimplified independent particle model of the increasingly neutron-rich nuclei [22]. The new rates lead to a smaller homologous core and to a lower initial shock energy at bounce [23]. On the other hand, weak magnetism corrections in the hot dissociated matter on the upper branch of Figure 2a have been added to zeroth-order cross sections [24]. This results in a slightly different balance between neutrinos and antineutrinos in the accretion phase for all three neutrino flavours [25].

The equation of state (EoS) is the second nuclear physics pillar of supernova simulations. It has to define composition and thermodynamic quantities as a function of density, entropy, and electron fraction over a wide range of conditions. Firstly, the EoS can directly influence the dynamics. A higher compressibility of matter at bounce, for example, leads to a larger initial shock energy [26]. Secondly, the composition is another important path for the EoS to affect the simulations. A composition with a high fraction of nuclei with large electron capture rates will lead to faster deleptonization than a composition with nuclei that forbid electron captures. Or, later in the accretion phase, a large fraction of alpha particles in the heating region will decrease the heating efficiency because they can not absorb neutrinos as efficiently as free nucleons. Thirdly, the EoS influences the simulations by the geometric arrangement of its consistutents. During collapse, the ions in the low-entropy matter are spatially correlated and coherence effects should be considered in the calculation of neutrino opacities ([27] and references therein). The phase transition from isolated nuclei to bulk nuclear matter is expected to involve complicated clustering of baryons that might affect neutrino opacities as well [28, 29, 30].

Finally, the EoS determines the simulation results by the macroscopic structure of the PNS in hydrostatic equilibrium. Even if the high opacity prevents the high-density regime of the PNS from affecting the simulations directly by neutrino transport, it is the compactness of the proto-neutron star which determines the positions of the neutrinospheres in the gravitational potential. The positions of the neutrinospheres have clearly visible consequences for the neutrino luminosity and spectrum. This became evident in simulations investigating GR effects [31, 16] as well as in simulations comparing different EoS's [32, 17].

4. Neutrino emission

The neutrino signal during collapse and the energetic neutronization burst few milliseconds after bounce are surprisingly similar for progenitor stars of 13 $M_\odot$ to 40 $M_\odot$. This is due to a similar size of the collapsing core at the point of gravitational instability and to negative feedback in the net deleptonization rate before neutrino trapping [25]. The neutrino luminosities during the accretion phase are more progenitor dependent. The diffusion of neutrinos out of the cooling PNS provides the dominant contribution to the μ- and τ-neutrino signal. An additional contribution (of about equal size) to the electron flavour neutrino luminosities stems from the compression of the hot accreted matter settling on the surface of the PNS. This

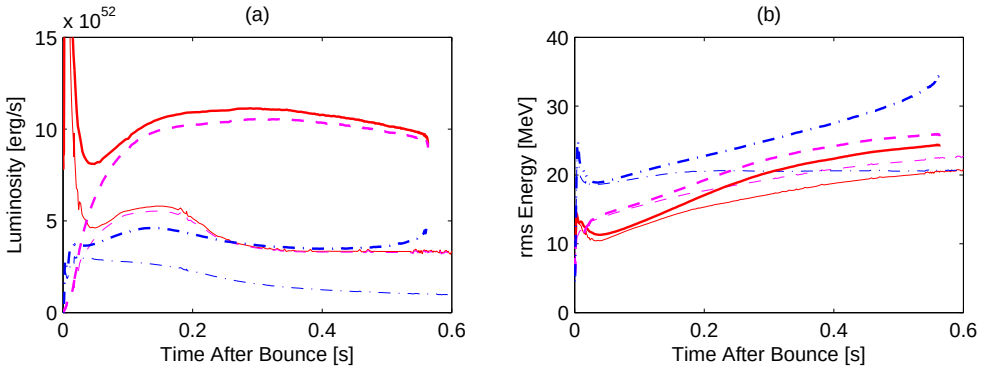

Figure 3. Shown are the neutrino luminosities and the rms energy of the neutrino fluxes as a function of postbounce time for two different progenitor stars: a $15M_\odot$ star [33] (thin lines) and a $40M_\odot$ star [34] (thick lines). The solid, dashed and dash-dotted lines refer to electron neutrinos, electron antineutrinos and heavy neutrinos respectively. The values are given at 200 km radius in the frame comoving with the fluid.

contribution depends strongly on the accretion rate.

Figure 3a shows the time evolution of the neutrino luminosities for two different progenitor stars after the decay of the neutronization burst. The thin lines correspond to an extension of model G15 [19]. While the luminosities of the heavy neutrinos (dash-dotted line) show a progressively cooling PNS, the electron flavor neutrinos (solid and dashed lines) reveal a significant drop in the accretion rate around 200 ms after bounce before they level off to an extended stationary accretion phase. This behaviour is expected for a PNS that does not compress significantly because it is quite far from reaching its maximum stable mass. Since μ- and τ-neutrino producing layers in the PNS cool faster than they are compressionally heated, the rms energies of the heavy neutrinos fall below the rms energies of the electron flavour neutrinos, which stem from the continued accretion of hot matter. The accretion rate would suddenly drop at the time of an eventual explosion (not obtained in this run). The electron flavour neutrino luminosities would then suddenly decay and asymptote to the level of the heavy neutrino luminosities of the cooling PNS.

A different scenario occurs for a 40 $M_\odot$ progenitor star [34] whose luminosities in the postbounce evolution are also displayed in Figure 3a (thick lines). We also see the decreasing accretion rate reflected in the electron flavour neutrino emission (solid and dashed lines), but the heavy neutrino luminosities go through a minimum and raise again (dash-dotted line). This is due to the hydrostatic compactification of the PNS as it approaches the maximum stable mass determined by the high-density EoS. Hot accreted matter is compressed to densities where the main μ- and τ-neutrino production takes place so that their luminosities increase [35, 36, 37]. We want to emphasize with this comparison that large differences in the neutrino luminosities (and spectra) in models for different explosion scenarios and launched from different progenitor models do not just classify as 'uncertainties', they reflect various dynamical processes at the center of a collapsed star, like the exact time of core-bounce, the evolution of the accretion rate, the compressibility of the PNS, the formation of a black hole, or the onset of the supernova explosion.

Before the neutrino signal reaches a terrestrial observer, one has to account for

neutrino flavour transformations. Of special interest for the neutrino heating after the onset of the explosion are possible collective modes [38, 39].

5. Spherical ejection models and nucleosynthesis

Supernova nucleosynthesis predictions traditionally rely on artificially induced explosions, replacing the central engine either with a parameterized kinetic energy piston or a thermal bomb. The explosion energy and the placement of the mass cut (separating ejected matter from matter which is assumed to fall back onto the neutron star) are tuned to recover the observed explosion energy and ejected ^{56}Ni mass. Both approaches are largely compatible [40] and justifiable for the outer stellar regions, but most of the Fe-group nuclei are produced in the inner regions which are most affected by the details of the explosion mechanism. The electron fraction Y_e is an indispensable quantity for the description of the explosive nucleosynthesis in the innermost ejecta. It is set by weak interactions in the explosively burning layers, i.e. electron and positron capture, beta-decays, and neutrino or anti-neutrino captures.

We examined the effects of both electron and neutrino captures in the context of spherically symmetric simulations with Boltzmann neutrino transport [20]. In order to provoke the ejection of matter in spherically symmetric models, we had to modify the simulations in the accretion phase. Having PNS convection [3] or convective turnover [4] in mind, we artificially enhanced the neutrino emission from the PNS or, alternatively, the neutrino absorption efficiency in the hot mantle surrounding it. Both approaches serve as matter ejection models with a consistently emerging mass cut. Similar simulations using tracer particles from two-dimensional simulations [13] have been performed in [41]. Also in this case, artificial adjustments to the simulations were needed to remedy the failure of the underlying models to produce self-consistent explosions. Also in both cases, the neutrino transport could not be run to later times and the simulations were mapped to a simpler model to continue the simulation. Despite these shortcomings, these simulations reveal the significant impact of neutrino interactions on the composition of the ejecta. At early times, the inner ejecta are electron-degenerate and electron capture dominates. Due to neutrino heating in the heating region and the expansion this degeneracy is lifted and electron-emitting neutrino absorption reactions start to dominate the change of Y_e. Eventually the electron chemical potential drops below the mass difference between the neutron and proton. At this energy scale, the proton is favored because of its slightly larger binding energy. We found that all our simulations that lead to an explosion by neutrino heating developed a proton-rich environment around the mass cut with $Y_e > 0.5$ [20].

The nucleosynthesis in proton-rich ejecta has been investigated in [42, 43, 41]. The global effect of the proton-richness is the removal of previously documented overabundances of neutron rich iron peak nuclei [33, 44]. Production of ^{58,62}Ni is suppressed while ^{45}Sc and ^{49}Ti are enhanced. The results for the elemental abundances of scandium, cobalt, copper, and zinc are closer to those obtained by observation [20]. However, the neutrino interactions are not only responsible for the proton-richness of the environment, they also transform protons into neutrons by antineutrino capture so that (n,p)-reactions substitute for the slow β-decays in the waiting point nuclei, allowing significant flow to $A > 64$ by the νp-process [45]. This process turns out to have a significant impact on the nucleosynthesis in the early neutrino wind [46, 47].

Acknowledgements

This work was supported in part by grants No. PP002-106627/1, No. 200020-105328/1 and No. IB7320-110996/1 from the Swiss National Science Foundation and the EU program ILIAS N6 ENTApP WP1.

References

[1] Baade W and Zwicky F 1934 *Proceedings of the National Academy of Science* **20** 259–63
[2] Bethe H A 1990 *Rev. Mod. Phys.* **62** 801–66
[3] Wilson J R and Mayle R W 1993 *Phys. Repts.* **227** 97–111
[4] Herant M, Benz W, Hix W R, Fryer C L and Colgate S A 1994 *ApJ* **435** 339–61
[5] Blondin J M, Mezzacappa A and DeMarino C 2003 *ApJ* **584** 971–80
[6] Foglizzo T, Galletti P, Scheck L, and Janka H-Th 2007 *ApJ* **654** 1006–21
[7] Burrows A, Livne E, Dessart L, Ott C D , and Murphy J 2006 *ApJ* **640** 878–90
[8] Kotake K, Sato K, and Takahashi K 2006 *Reports of Progress in Physics* **69** 971–1143
[9] Liebendörfer M, Pen U-L and Thompson C 2006 In *Proceedings of Science* PoS(NIC-IX)132
[10] Lattimer J M and Swesty F D 1991 *Nucl. Phys. A* **535** 331–76
[11] Liebendörfer M 2005 *ApJ* **633** 1042–51
[12] Hamuy M 2003 *ApJ* **582** 905–14
[13] Buras R, Rampp M, Janka H-Th and Kifonidis K 2003 *Phys. Rev. Lett.* **90** 241101
[14] Walder R, Burrows A, Ott C D, Livne E, Lichtenstadt I and Jarrah M 2005 *ApJ* **626** 317–32
[15] Wilson J R 1971 *ApJ* **163** 209
[16] Liebendörfer M, Mezzacappa A, Thielemann F-K, Messer O, Hix W R and Bruenn S W 2001 *Phys. Rev. D* **63** 103004
[17] Sumiyoshi K, Yamada S, Suzuki H, Shen H, Chiba S and Toki H 2005 *ApJ* **629** 922–32
[18] Marek A, Dimmelmeier H, Janka H-Th, Müller E and Buras R 2006 *A&A* **445** 273–89
[19] Liebendörfer M, Rampp M, Janka H-Th and Mezzacappa A 2005 *ApJ* **620** 840–60
[20] Fröhlich C *et al* 2006 *ApJ* **637** 415–26
[21] Bruenn S W 1985 *ApJS* **58** 771–841
[22] Langanke K *et al* 2003 *Phys. Rev. Lett.* **90** 241102
[23] Hix W R, Messer O, Mezzacappa A, Liebendörfer M, Sampaio J, Langanke K, Dean D J and Martínez-Pinedo G 2003 *Phys. Rev. Lett.* **91** 201102
[24] Horowitz C J 2002 *Phys. Rev. D* **65** 043001
[25] Liebendörfer M, Mezzacappa A, Messer O, Martinez-Pinedo G, Hix W R, and Thielemann F-K 2003 *Nucl. Phys. A* **719** 144–52
[26] Bruenn S W 1989 *ApJ* **341** 385–400
[27] Marek A, Janka H-Th, Buras R, Liebendörfer M and Rampp M 2005 *A&A* **443** 201–10
[28] Watanabe G, Sato K, Yasuoka K and Ebisuzaki T 2004 *Phys. Rev. C* **69** 055805
[29] Horowitz C J, Pérez-García M A and Piekarewicz J 2004 *Phys. Rev. C* **69** 045804
[30] Botvina A S and Mishustin I N 2004 *Phys. Lett. B* **584** 233–40
[31] Bruenn S W, De Nisco K R, and Mezzacappa A 2001 *ApJ* **560** 326–38
[32] Janka H-Th, Buras R, Kitaura Joyanes F S, Marek A, Rampp M and Scheck L 2005 *Nucl. Phys. A* **758** 19–26
[33] Woosley S E and Weaver T A 1995 *ApJS* **101** 181
[34] Umeda H, Nomoto K, Kobayashi N and Tominaga N 2006 private communication
[35] Liebendörfer M, Messer O, Mezzacappa A, Bruenn S W, Cardall C Y and Thielemann F-K 2004 *ApJS* **150** 263–316
[36] Fischer T, Liebendörfer M and Mezzacappa A 2007 *J. of Phys. Conf. Ser.* **66** 2043
[37] Sumiyoshi K, Yamada S and Suzuki H 2007 *ArXiv e-prints* 0706.3762
[38] Duan H, Fuller G M and Qian Y-Z 2006 *Phys. Rev. D* **74** 123004
[39] Fogli G L, Lisi E, Marrone A and Mirizzi A 2007 *ArXiv e-prints* 0707.1998
[40] Aufderheide M B, Baron E and Thielemann F-K 1991 *ApJ* **370** 630–42
[41] Pruet J, Woosley S E, Buras R, Janka H-Th and Hoffman R D 2005 *ApJ* **623** 325–36
[42] Thielemann F-K *et al* 2002 *Space Sci. Rev.* **100** 277–96
[43] Umeda H and Nomoto K 2005 *ApJ* **619** 427–45
[44] Thielemann F-K, Nomoto K and Hashimoto M 1996 *ApJ* **460** 408–36
[45] Fröhlich C *et al* 2006 *Phys. Rev. Lett.* **96** 142502
[46] Pruet J, Hoffman R D, Woosley S E, Janka H-Th and Buras R 2006 *ApJ* **644** 1028–39
[47] Wanajo S 2006 *ApJ* **647** 1323–40